UCSF
UC San Francisco Previously Published Works

Title
CD36 Repression Activates a Multicellular Stromal Program Shared by High Mammographic Density and Tumor Tissues

Permalink
https://escholarship.org/uc/item/27p4t4vj

Journal
Cancer Discovery, 2(9)

ISSN
2159-8274

Authors
DeFilippis, Rosa Anna
Chang, Hang
Dumont, Nancy
et al.

Publication Date
2012-09-01

DOI
10.1158/2159-8290.cd-12-0107

Peer reviewed

eScholarship.org Powered by the California Digital Library
University of California

NIH Public Access

Author Manuscript

Cancer Discov. Author manuscript; available in PMC 2013 September 01.

Published in final edited form as:

Cancer Discov. 2012 September ; 2(9): 826–839. doi:10.1158/2159-8290.CD-12-0107.

CD36 Repression Activates a Multicellular Stromal Program Shared by High Mammographic Density and Tumor Tissues

Rosa Anna DeFilippis[1,2], **Hang Chang**[3], **Nancy Dumont**[1,2], **Joseph T. Rabban**[1], **Yunn-Yi Chen**[1], **Gerald V. Fontenay**[3], **Hal K. Berman**[4], **Mona L. Gauthier**[4], **Jianxin Zhao**[1,2], **Donglei Hu**[5], **James J. Marx**[6], **Judy A. Tjoe**[6], **Elad Ziv**[5], **Maria Febbraio**[7], **Karla Kerlikowske**[5,8], **Bahram Parvin**[3], and **Thea D. Tlsty**[1,2,*]

[1]Department of Pathology, University of California San Francisco, San Francisco, CA 94143, USA

[2]Comprehensive Cancer Center, University of California San Francisco, San Francisco, CA 94143, USA

[3]Lawrence Berkeley National Laboratory, Berkeley, CA, 94720, USA

[4]Department of Laboratory Medicine and Pathobiology, University of Toronto, Toronto, Ontario, Canada

[5]Department of Medicine, University of California San Francisco, San Francisco, CA 94143, USA

[6]Department of Patient Centered Research, Division of Breast Oncology, Aurora Health Care, Milwaukee, WI, 53233, USA

[7]Department of Molecular Cardiology, Lerner Institute, Cleveland Clinic Foundation, Cleveland, OH, 44195, USA

[8]Departments of Epidemiology and Biostatistics, University of California San Francisco, San Francisco, CA 94143, USA

Abstract

Although high mammographic density (MD) is considered one of the strongest risk factors for invasive breast cancer, the genes involved in modulating this clinical feature are unknown. Tissues of high MD share key histological features with stromal components within malignant lesions of tumor tissues, specifically low adipocyte and high ECM content. We show that CD36, a transmembrane receptor that coordinately modulates multiple pro-tumorigenic phenotypes including adipocyte differentiation, angiogenesis, cell-ECM interactions, and immune signaling, is greatly repressed in multiple cell types of disease-free stroma associated with high MD and tumor stroma. Using both *in vitro* and *in vivo* assays, we demonstrate that CD36 repression is necessary and sufficient to recapitulate the abovementioned phenotypes observed in high MD and tumor tissues. Consistent with a functional role for this coordinated program in tumorigenesis, we observe that clinical outcomes are strongly associated with CD36 expression.

Keywords

breast cancer; cell-cell interactions; CD36; mammographic density; stroma

---

*Corresponding author: Thea D. Tlsty, University of California San Francisco, 513 Parnassus, HSW 513, San Francisco, CA 94143, Phone: (415)-502-6115, Fax: (415)-502-6163, Thea.Tlsty@ucsf.edu.

No conflicts of interest

Detailed experimental procedures are included in Supplemental Materials and Methods.

NIH-PA Author Manuscript

NIH-PA Author Manuscript

NIH-PA Author Manuscript

NIH-PA Author Manuscript NIH-PA Author Manuscript NIH-PA Author Manuscript

Introduction

Many tissues are composed of an epithelium associated with a stroma that is comprised of ECM proteins, adipocytes, fibroblasts, endothelial, neuronal and immune cells. Fibroblasts, a major stromal cell type, produce many components of the ECM, as well as proteases that remodel it (1). Additionally, fibroblast signaling is a critical determinant of epithelial and stromal cell fate during development and differentiation (2), tissue homeostasis and wound healing (1).

Stromal changes associated with malignant lesions are heterogeneous and range from tumor suppressing to tumor promoting. Tumors, sub-typed by marker expression in epithelial cells, can be further categorized by their stromal signature, which dictates good or poor outcome (3). Fibroblasts within the stroma of malignant lesions, called carcinoma-associated fibroblasts (CAFs), differ from their counterparts in disease-free tissue (4). CAFs can stimulate tumor progression of initiated non-tumorigenic epithelial cells, both *in vitro and in vivo*, while normal fibroblasts cannot (5). CAFs increase proliferation and decrease apoptosis in adjacent epithelial cells and promote angiogenesis by recruiting endothelial progenitor cells into tumors (5, 6). All other stromal components, including immune and endothelial cells, also participate in malignant progression (4).

The stroma within, and immediately adjacent to, a malignant lesion may exhibit a range of histologic alterations, called desmoplasia. The alterations range from a predominantly cellular stroma, containing fibroblasts, vascular and immune cells with little ECM, to a dense tissue with a minimum of cells and a maximum content of matrix (4, 7). Additionally, tumor stroma exhibits a reduction in the size and number of adipocytes (8). The most odious stromal changes include extreme ECM deposition and remodeling along with aberrant vasculature and fibroblast and immune cell infiltration. Classically, participation of the stroma has been viewed as a reactive process, where signals from malignant epithelial cells recruit and stimulate these stromal components.

Interestingly, some desmoplastic features are seen in cancer-free tissues of women at high risk for breast cancer, namely in the context of wound healing, radiation response, pregnancy-associated involution and high mammographic density (MD) (4, 8–10). MD is of particular interest since almost 1/3 of breast cancers are thought to be attributable to phenotypes associated with high breast density, MD being a strong risk factor with high prevalence (11, 12). MD is determined by the relative amounts of radiolucent material (fat) and radio-dense material (epithelial cells, fibroblasts and connective tissue) within the breast on a mammogram, either of which may occupy anywhere between 0 and 100% of the gland. Radio-dense areas exhibit several histological characteristics of stroma associated with malignant epithelial cells, specifically low adipocyte content and high ECM and stromal cell content (9, 10). Epidemiological studies suggest that women with high MD have a 4- to 6-fold increase in risk for invasive breast cancer compared to women with low MD (11, 13–15).

Studies comparing pairs of monozygotic and dizygotic twins attributed 53–67% of the variation in MD to heritable factors with the remaining portion modulated by environmental or physiological factors (16–21). For example, post-menopausal hormone therapy increases MD in some women, while tamoxifen treatment decreases MD in both pre- and post-menopausal women and subsequently modulates breast cancer risk (19, 21). This modulation by exogenous factors provides an exciting opportunity for intervention and prevention.

NIH-PA Author Manuscript

NIH-PA Author Manuscript

NIH-PA Author Manuscript

Boyd and co-workers examined the molecular composition of low and high MD tissues (9, 10) and report higher levels of insulin like growth factor-I (IGF-I) and tissue inhibitor of metalloproteinase 3 (TIMP-3) in high MD tissue. Recent studies found additional changes including differences in estrogen and prostaglandin metabolism and TGFβ signaling (22–24). While these studies begin to define the molecular constituents of MD that may explain the basis of high MD and its association with increased breast cancer risk, they are correlative and thus cannot demonstrate that these genes or proteins mechanistically modulate phenotypes of MD.

The observation of multiple desmoplastic phenotypes in tissues of high MD, in the absence of a tumor, strongly suggests that these stromal phenotypes are not simply part of a reactive response to existing tumor cells, but also represent a program involving multiple stromal components that may create a proactive milieu for the emergence or progression of cancer. Therefore, we hypothesized that the phenotypes observed in both high MD and tumor stroma may be controlled by a common molecular program and thus their stromal components would share phenotypic, molecular and functional characteristics.

Here we demonstrate that the level of expression of a single molecule, CD36, is necessary and sufficient to simultaneously control adipocyte content and matrix accumulation, two phenotypes shared by desmoplasia and high MD. CD36, a widely expressed transmembrane receptor, modulates cell type- and ligand-specific phenotypes including adipocyte differentiation, angiogenesis, apoptosis, TGFβ activation, cell-ECM interactions, and immune signaling (25). We found that CD36 expression was negligible in multiple cell types of tumor stroma compared to surrounding histologically disease-free tissue. Strikingly, high MD tissues, devoid of any malignancy, also showed reduced CD36 levels in multiple cell types compared to low MD tissues. The low level of CD36 expression shared by high risk (but cancer-free) and malignant tissues suggests that it constitutes a causal and very early event in generating the distinctive characteristics of a tumor stroma.

Results

Desmoplasia and tissues with high MD share histologic characteristics

The appearance of stroma associated with malignant epithelial cells is strikingly different from the appearance of most stroma associated with disease-free ductal tissue. Increases in ECM, endothelial and immune components, and the absence of adipocytes, are obvious upon inspection (Figure 1). Strikingly, similar stromal alterations are observed histologically in disease-free tissue of women with high MD as compared with women with low MD, specifically low adipocyte and high ECM content (Figure 1). We examined fibroblasts from tissue of high and low MD, as well as from tumor tissue, for phenotypic similarities that may underlie their shared histologic appearance.

HDAFs and LDAFs recapitulate phenotypes of high and low MD tissues, respectively, *in vitro*

To determine if fibroblasts obtained from low and high MD tissues and propagated *in vitro* could recapitulate the two prominent *in vivo* phenotypic differences described above, low density associated fibroblasts (LDAFs) and high density associated fibroblasts (HDAFs) were purified from disease-free breast biopsies from women with 25–50% MD and women with >75% MD, respectively (Supplementary Table S1). LDAFs and HDAFs were placed under proliferative or adipocyte differentiation conditions for 6 days prior to assessing their ability to accumulate fat by Oil Red O staining (Figure 2A). Fat accumulation was quantitated on a cell-by-cell basis as previously described (Supplementary Figure S1) (26). This analysis showed that, while both LDAFs and HDAFs accumulated fat under

NIH-PA Author Manuscript

NIH-PA Author Manuscript

NIH-PA Author Manuscript

differentiation conditions (10.0-fold and 5.6-fold, respectively, $p<10^{-8}$), HDAFs accumulated significantly less fat (3.1-fold, $p<10^{-8}$) than LDAFs (Figure 2B). This decrease in the average amount of fat accumulation per cell was due to a decrease in both the percentage of cells that contain fat and the amount of fat per cell (Supplementary Figure S2).

To determine whether LDAFs and HDAFs differed in their adipocyte differentiation capacity, rather than simply fat storage, the expression levels of CD36 and leptin (LEP) (previously reported to be up-regulated during adipocyte differentiation) (27) were measured by quantitative PCR (Q-PCR) in cells grown under proliferative or adipocyte differentiation conditions for 2 weeks. Both LDAFs and HDAFs could undergo adipocyte differentiation, however LDAFs showed higher levels of expression of CD36 and LEP compared to HDAFs (CD36: 2.7-fold, p=0.03; LEP: 6.8-fold, p=0.05) (Figure 2C). These data demonstrate that differences in fat accumulation between LDAFs and HDAFs is due to differences in their adipocyte differentiation capabilities.

Having demonstrated that cultured LDAFs and HDAFs recapitulated their respective *in vivo* adipocyte phenotypes, we examined whether they could also recapitulate their *in vivo* matrix accumulation phenotypes in a short-term assay. LDAF and HDAF cultures were probed after 5 days of propagation for accumulation of matrix proteins known to be increased in desmoplasia: collagen 1A1 (COL1A1), fibronectin (FN1), osteopontin (OPN) and tenascin C (TNC) (1) (Supplementary Figure S3). Cell-by-cell immunofluorescence quantitative analysis (Supplementary Figure S1) revealed heterogeneity within the cultures with an overall small but statistically significant greater amount of COL1A1, FN1 and OPN (each 1.1-fold, $p<10^{-8}$) in HDAFs compared to LDAFs (Figure 2D). However, HDAFs accumulated a statistically significant lesser amount of TNC (1.1-fold, $p<10^{-8}$) than LDAFs, suggesting that there is not a global increase in all matrix protein accumulation (Figure 2D). One could speculate that this modest increase in matrix accumulation over a prolonged period of time (years), in contrast to our 5-day assay, could account for the dramatic differences observed *in vivo*.

CAFs recapitulate phenotypes of desmoplasia *in vitro*

CAFs have been shown to promote ECM deposition *in vitro* and *in vivo*, but little is known concerning their ability to modulate adipocyte differentiation (1). To this end, human mammary fibroblasts purified from invasive cancer tissues (CAFs) and from reduction mammoplasty tissues (RMFs) (Supplementary Table S2) were assayed as above for fat accumulation (Figure 2E, **left panel**). Cell-by-cell quantitation of Oil Red O staining (Supplementary Figure S1) showed that, while both RMFs and CAFs accumulated fat under differentiation conditions (27-fold and 8-fold, respectively, $p<10^{-8}$), CAFs were deficient in fat accumulation compared to RMFs (5.8-fold, $p<10^{-8}$) (Figure 2E, **right panel**).

CD36 expression is decreased in fibroblasts from high mammographic density and tumor tissues

To gain insight into the molecular basis for these phenotypes, gene expression profiling was used to identify genes differentially expressed between LDAFs and HDAFs (GEO GSE38506). CD36 showed the largest difference, its expression being down-regulated 3.7–4.3-fold in HDAFs relative to LDAFs (Supplementary Table S3). In order to validate these microarray results, CD36 transcript and protein levels were measured in LDAFs and HDAFs by Q-PCR and Western blot analysis. Both CD36 gene expression (8.6-fold, p=0.002) and protein levels were decreased in HDAFs relative to LDAFs (Figure 3A&B).

Given the striking down-regulation of CD36 in fibroblasts of high MD, we examined CD36 expression in fibroblasts isolated from malignant tissue and in microarrays of tumor tissue.

NIH-PA Author Manuscript

CD36 expression, measured by QPCR, was decreased 4.3-fold (p=0.001) in CAFs relative to RMFs (Figure 3C). Similarly, analysis of 6 independent public gene expression datasets (Supplementary Table S4) consistently showed a statistically significant decrease in CD36 expression in invasive ductal carcinoma (IDC) tissues compared to normal tissues (3.6 to 12.3-fold). In light of the striking repression of CD36 in fibroblasts from high MD and tumor tissues, we examined the role of CD36 in modulating the two prominent *in vivo* phenotypes shared by these tissues: decreased adipocyte content and increased matrix accumulation (4, 8–10).

CD36 expression is necessary and sufficient to modulate adipocyte differentiation and matrix accumulation *in vitro*

Little is known about the basis of decreased adipocyte content in high MD and desmoplastic tissues. However, induction of CD36 expression is necessary for proper adipocyte differentiation in pre-adipocytes (28) and serves as a marker for terminal differentiation (27). To determine if CD36 expression could modulate adipocyte content, we genetically modulated CD36 levels in RMFs selected for their intermediate baseline expression level of CD36. To determine if CD36 expression was necessary for fat accumulation, CD36 expression was repressed in RMFs by transduction of lentiviral particles expressing short hairpin RNA to CD36 (shCD36) (Supplementary Figure S4). Cell-by-cell quantitation of Oil Red O staining (Supplementary Figure S1) showed that, while both control (shLuc) and shCD36 cells accumulated fat under differentiation conditions (8.9-fold and 3.1-fold, respectively, $p<10^{-8}$), control cells accumulated significantly more fat than shCD36 cells (6.1-fold, $p<10^{-8}$) (Figure 4A). These data demonstrate that CD36 is necessary for fat accumulation. To determine if CD36 expression was sufficient for fat accumulation, CD36 expression was increased in RMFs by transduction of lentiviral particles expressing CD36 (CD36 OE) (Supplementary Figure S4). Cell-by-cell quantitation of Oil Red O staining (Supplementary Figure S1) showed that, while both control (vector) and CD36 OE cells accumulated fat under differentiation conditions (2.2-fold and 4.7-fold, respectively, $p<10^{-8}$), CD36 OE cells accumulated significantly more fat than control cells (3.3-fold, $p<10^{-8}$) (Figure 4B). These data demonstrate that CD36 is sufficient for fat accumulation. Therefore, the decrease in CD36 expression in HDAFs and CAFs could account for their reduced ability to accumulate fat compared to LDAFs and RMFs, respectively.

In order to determine if CD36 expression could also modulate matrix accumulation, the fibroblasts with genetically modulated levels of CD36 described above were probed for the accumulation of matrix proteins known to be increased in HDAFs: COL1A1, FN1, and OPN (Figure 4C). Cell-by-cell immunofluorescence quantitative analysis (Supplementary Figure S1) revealed that cells with low CD36 (shCD36) accumulated a statistically significant greater amount of COL1A1, FN1 and OPN (1.6-fold, 2.8-fold and 1.7-fold, respectively, $p<10^{-8}$) compared to control cells (shLuc) (Figure 4D, **left panel**). Conversely, cells with high CD36 (CD36 OE) accumulated a statistically significant lesser amount of COL1A1, FN1 and OPN (1.4-fold, 2.1-fold and 1.3-fold, respectively, $p<10^{-8}$) compared to control cells (vector) (Figure 4D, **right panel**). Of particular note, these changes in matrix accumulation were already observed after only 5 days of culture. These data demonstrate that reduced CD36 expression is necessary and sufficient for increased matrix accumulation. Taken together, the decreased CD36 expression seen in high MD and tumor tissues can result in the coordinated decrease in fat accumulation and increase in matrix accumulation observed *in vivo*.

Cd36 knockout mice phenocopy human high MD and desmoplastic tissues

In order to determine whether the modulation of fat and matrix accumulation by CD36, which we observed *in vitro,* also occurs *in vivo*, we compared characteristics of fat and

NIH-PA Author Manuscript

NIH-PA Author Manuscript

NIH-PA Author Manuscript

matrix accumulation in mammary glands of wild type (WT) and Cd36 knockout (CD36 KO) mice (29). Paraffin sections of the #4 mammary glands of WT or CD36 KO mice were stained with Masson's Trichrome, imaged (Figure 5A) and quantitated on a cell-by-cell (for fat analysis) or image-by-image (for matrix analysis) basis (Supplementary Figure S1). CD36 KO mice exhibited a statistically significant decrease (1.2-fold, $p<10^{-8}$) in fat accumulation (fat cell area) (Figure 5B) and a statistically significant increase (2.1-fold, $p<10^{-8}$) in matrix accumulation (Figure 5C) relative to WT mice. Paraffin sections were stained for COL1A1 and FN1 (Figure 5D&E, **left panels**), two matrix proteins modulated by CD36 *in vitro* (Figure 4C&D). Image-by-image quantitative analysis (Supplementary Figure S1) revealed that CD36 KO mice accumulated a statistically significant greater amount of COL1A1 and FN1 (both 1.6-fold, $p<10^{-8}$ and $p=5.5\times10^{-7}$, respectively) compared to WT mice (Figure 5D&E, **right panels**). Therefore CD36 KO mice exhibited two prominent phenotypes of high MD and desmoplastic tissues in women: decreased fat accumulation and increased matrix accumulation, demonstrating causality between CD36 expression and modulation of both phenotypes *in vitro* and *in vivo*.

CD36 expression is decreased in multiple cellular compartments of high MD tissues compared to low MD tissues

CD36 is expressed on the surface of many cells that reside within tissue stroma, but not on epithelial cells (25). Given that microarray analysis of whole tumor tissues showed a dramatic reduction in CD36 compared to disease-free tissues (Supplementary Table S4), we determined if cellular components other than fibroblasts also exhibited a repression of CD36. Tissue sections from core or excisional biopsies, obtained from cancer-free women with either low MD (LD) or with high MD (HD) (Supplementary Table S5), were stained for CD36 (Supplementary Figure S5) and imaged (Figure 6A, **left panels**). As expected, adipocytes, endothelial cells, macrophages and fibroblasts each stained positive for CD36, while epithelial cells did not. However, a striking decrease in the intensity of CD36 staining in the high MD tissues was observed in every cell type noted above, indicating that CD36 repression reflects a widespread multi-cellular program. CD36 positive staining was measured on a cell-by-cell basis as previously described (26) (Supplementary Figure S1). The average amount of CD36 staining per cell was lower in HD tissues compared to LD tissues (4.5-fold, $p<10^{-8}$) (Figure 6A, **right panel**) due to a decrease in both the percentage of CD36-positive cells and the intensity of CD36 staining per cell (Supplementary Figure S6).

CD36 expression is decreased in multiple cells types within the stroma of malignant lesions compared to histologically normal adjacent tissues

Having observed that CD36 expression is decreased in multiple cell types within tissues of high MD, we investigated whether the same would be true in tumor tissues obtained from women with estrogen receptor (ER)/progesterone receptor (PR)-positive, HER2-positive or ER/PR/HER2-negative (triple negative (TN)) invasive ductal cancer (IDC) (Supplementary Table S6). Tissue sections from this cohort were stained for CD36 and imaged in both the tumor (CA) field and the histologically normal adjacent (NA) areas (Figure 6B). In all tumor subtypes, CD36 expression was strikingly absent in the tumor field compared to the NA tissue (Figure 6B). Cell-by-cell quantitation of CD36 staining (Supplementary Figure S1) revealed that CD36 expression was reduced 14.7-fold ($p<10^{-8}$) in tumor tissue compared to NA tissue (Supplementary Figure S7). This was due to a decrease in both the percentage of CD36-positive cells and the intensity of CD36 staining per cell (Supplementary Figure S6). A similar dramatic decrease in CD36 expression was observed in each tumor subtype (Figure 6C). Notably, it has been reported that women with high MD have a higher propensity to develop ER-negative tumors compared to women with low MD (30). Strikingly, NA tissue from TN (ER-negative) tumors exhibited significantly lower levels of

NIH-PA Author Manuscript

NIH-PA Author Manuscript

NIH-PA Author Manuscript

CD36 expression compared to ER+ or HER2+ tumors (Figure 6C). Taken together, these data suggest that low expression levels of CD36, as seen in tissues with high MD, may predispose a subset of women to develop TN tumors, a tumor subtype associated with poor disease outcome.

To identify the cellular basis of the reduced CD36 staining, we examined the cells that typically express CD36 in histologically normal tissues (adipocytes, endothelial cells and macrophages). Although scarce, adipocytes within tumor tissue not only showed decreased expression of CD36, but were also smaller in size compared to adipocytes adjacent to the tumor (Supplementary Figure S7). Staining of serial sections for endothelial and macrophage markers CD31 and CD68, respectively, revealed that endothelial cells and macrophages were still present within the field of tumor tissue, albeit with repressed CD36 expression (Supplementary Figure S7). In contrast, in the NA tissue, endothelial cells and macrophages positive for CD31 and CD68, respectively, also stained positive for CD36 (Supplementary Figure S7). Together with the results in Figure 3C, these data demonstrate that CD36 expression is actively repressed in fibroblasts, adipocytes, endothelial cells and macrophages within tumor tissue compared to normal adjacent tissue. This documents that CD36 repression in tumor tissue, also seen in high MD tissue, reflects a widespread, coordinated, multi-cellular program.

The repression of CD36 in multiple cell types in high MD tissue compared to low MD tissue, in the absence of a tumor, suggests that this repression can be an early event that precedes overt tumor formation. If this were the case, one might predict that CD36 levels would be repressed in histologically normal tissue directly adjacent to the tumor compared to histologically normal tissue distal to the tumor. To test this hypothesis, multiple tissue sections containing both tumor (CA) and histologically normal adjacent tissue (NA) or histologically normal distal tissue (ND, >40 mm away from the tumor) were obtained from 3 women with invasive cancer (Supplementary Table S7 **and** Figure S8). Tissue sections were stained for CD36, imaged in the CA, NA and ND fields (Figure 7A–C, **left panels**) and quantified for CD36 expression on a cell-by-cell basis (Supplementary Figure S1). In accordance with the results reported above, CD36 expression was reduced in CA compared to NA and ND tissues in all 3 women (4.7-fold to 113-fold and 6.8-fold to 159-fold, respectively, $p<10^{-8}$) (Figure 7A–C, **right panels**). Consistent with the hypothesis above, we observed in two out of three cases, that the NA tissue exhibited CD36 repression compared to its matched ND tissue (1.4-fold, $p<10^{-8}$) (Figure 7A&B). In further support of this interpretation, it has been reported that invasive cancers often develop in regions previously measured as radio-dense for many years prior to tumor detection (31). Interestingly, one sample did not show this difference between NA and ND tissues (Figure 7C). A more detailed analysis of this heterogeneity is currently under investigation.

Clinical outcome is associated with CD36 expression

Given the dramatic universal repression of CD36 observed within the stroma of all tumor subtypes examined (Figure 6B&C), we determined if the initial CD36 levels in non-diseased breast tissue (i.e. MD) would stratify tumors for their ultimate CD36 repression and subsequent clinical phenotypes. Tissue sections containing tumor tissue, obtained from women with low MD (LD) and women with high MD (HD) diagnosed with ER positive IDC (Supplementary Table S8), were stained for CD36 and imaged (Figure 6D, **left panels**). As expected, CD36 staining was very low in all tumor tissues. However, using cell-by-cell quantitation (Supplementary Figure S1), the average amount of CD36 staining per cell was lower in the tumor tissues of women with high MD compared to women with low MD (1.7-fold, $p<10^{-8}$) (Figure 6D, **right panel**). This was due to a decrease in both the percentage of CD36-positive cells and the intensity of CD36 staining per cell (Supplementary Figure S6).

NIH-PA Author Manuscript

NIH-PA Author Manuscript

NIH-PA Author Manuscript

Women with high MD who develop invasive cancer have an increased risk for aggressive disease, in that they develop larger tumors of more advanced-stage and higher grade, compared to women with low MD (30, 32, 33). Since CD36 expression is reduced in tissues of high MD, we examined whether CD36 expression was correlated with tumor grade and size. We interrogated CD36 expression in two public gene expression datasets (GSE6532 and GSE9195) for which molecular and associated clinical data were available for tumor samples from a total of 398 treatment-naïve IDC patients (34, 35). We analyzed tumor grade, tumor size and age as a function of CD36 expression using linear regression analyses (Supplementary Table S9). For the purpose of this analysis, we transformed CD36 levels so that they approximated a standard normal distribution (mean~0, standard deviation (SD)~1). These analyses revealed a statistically significant inverse relationship between CD36 expression and tumor grade and, independently, tumor size. CD36 expression was reduced 0.38 SD ($p=0.007$) in poorly-differentiated tumors (grade 3) compared to well-differentiated tumors (grade 1), after adjusting for the association between CD36 expression and tumor size. In addition, CD36 expression was reduced 0.15 SD ($p=0.003$) for every 1cm increase in tumor size, after adjusting for the association between CD36 expression and tumor grade. There was no significant association between CD36 expression and age.

In sum, stromal characteristics prior to tumor formation, in this case reflected by extent of MD and CD36 expression levels, are associated with clinical outcome.

Discussion

Using a combination of *in vitro* cell assays and *in vivo* screening of human and murine mammary tissue samples, we demonstrate that the level of expression of a single molecule, CD36, is necessary and sufficient to simultaneously control adipocyte content and matrix accumulation, two phenotypes which histologically define MD. This is the first report of a gene shown to mechanistically modulate selected phenotypes of MD. An important and novel finding of our study is that repression of CD36 is observed in both stroma associated with a malignant lesion and in breast tissue with high MD in the absence of malignancy. Equally important is our demonstration that repression of CD36 is not limited to a specific cell type but rather is observed in all stromal components, as documented here for adipocytes, endothelial cells, macrophages and fibroblasts, thus highlighting that expression of CD36 is part of a complex coordinated multi-cellular program. Taken together, these data suggest that expression of this stromal program is not only a reactive response to existing tumor cells but also represents a physiological state that increases cancer risk. Our data suggest a functional role for this coordinated program since the more repressed CD36 expression is, the more aggressive the tumor.

CD36 is uniquely poised to coordinately orchestrate distinct pro-tumorigenic phenotypes involving multiple cell types. In endothelial cells, where CD36 blocks VEGF-induced proliferation, migration and sprouting as well as induces apoptosis in response to ligand binding, its reduced expression could promote a pro-angiogenic phenotype (36, 37). In activated macrophages, where CD36 promotes the formation of foam cells and atherosclerotic plaques, triggers the release of inflammatory cytokines and reactive oxygen species (ROS), and inhibits migration (25), its reduced expression could induce multiple, potentially pro-tumorigenic, phenotypes. In support of this, macrophages from CD36 KO mice have reduced levels of ROS, iNOS and inflammatory cytokines (including IFN-γ and TNF-α) and increased arginase activity (38), indicative of a shift from an M1 pro-inflammatory/anti-tumorigenic state to an M2 anti-inflammatory/pro-tumorigenic state (39). In dendritic cells, where CD36 normally mediates the uptake of apoptotic cells and the cross-presentation of tumor-specific antigens to cytotoxic T cells (25), its reduced expression could allow the tumor to evade the immune system (40). The decreased

NIH-PA Author Manuscript

NIH-PA Author Manuscript

NIH-PA Author Manuscript

adipocyte differentiation (with reduced adiponectin (Apn)) and increased matrix accumulation (with increased collagen (Col1a1)) that we observed with reduced CD36 expression *in vitro* and *in vivo* have been shown to cause an increase in tumor burden, angiogenesis and metastasis in a murine mammary tumor model (MMTV-PyMT mice crossed with Apn KO or Col1a1^{tmJae} mice, respectively) (41, 42). Finally, increased matrix accumulation could stiffen the microenvironment, thereby potentially altering mechano-sensory networks involved in differentiation and malignancy (43, 44). In light of the central role of CD36 in modulating many functions in multiple cell types, one would predict that the reduction of CD36 expression could have widespread consequences.

The pro-oncogenic tissue state created by repression of CD36 goes far beyond merely supporting the malignant program of a transformed epithelial cell; it creates an interactive milieu that actively participates in tumorigenesis. Hence, our study provides novel insights into a molecular program that controls several stromal phenotypes underlying tumorigenesis. The "single hit, multiple target" nature of CD36, similar to micro-RNAs, makes it a very attractive therapeutic target. Moreover, in light of its role in MD, strategies to modulate CD36 have the potential to prevent cancer progression in women who are at high risk. In support of this, we demonstrate that increased expression of CD36 can restore stromal phenotypes associated with low risk tissues (Figure 4). Promisingly, expression of CD36 can be increased *in vitro* by treatment with aspirin, dexamethasone, statins or Adalimumab and *in vivo* by treatment with tamoxifen (45–49). Finally, MD can also be modulated by a variety of exogenous agents such as hormones, tamoxifen and diet. As such, MD represents a highly promising target for intervention as well as a biomarker that can assess response to prevention interventions (19, 21).

Materials and Methods

Isolation and propagation of human mammary fibroblasts (HMFs)

Fibroblasts were isolated from reduction mammoplasty, low and high MD, or tumor tissues and assessed for purity as described (5).

Microarray and quantitative PCR (QPCR) analysis

Total RNA, isolated from fibroblasts subjected or not to adipocyte differentiation, was used to generate cDNA using TaqMan Reverse Transcription Reagents (Applied Biosystems). The cDNA was used for Q-PCR (TaqMan) using the standard curve method with primer probe sets for CD36 and leptin. Expression of beta-D-glucuronidase (GUSB) was used to normalize input cDNA. For microarray experiments, mRNA, amplified and biotinylated from total RNA obtained from LDAFs and HDAFs using the MessageAmp II Kit (Ambion), was fragmented and hybridized to HU133 plus 2 chips (Affymetrix).

Adipocyte differentiation assay

Fibroblasts, plated at near confluency and grown for 48 hours, were treated with 10μM 15-deoxy-$\Delta^{12,14}$-Prostaglandin J2 (PJ2, Cayman Chemical) to induce adipocyte differentiation. Lipid accumulation was assayed by Oil Red O staining. Adipocyte differentiation was assessed by monitoring CD36 and leptin expression after 2 weeks of treatment.

Matrix accumulation

Fibroblasts, plated at near confluency into 8 well glass chamber slides, were grown for 5 days. Matrix accumulation was assessed by monitoring expression of collagen 1A1 (COL1A1, Abcam), fibronectin (FN1, BD Biosciences), osteopontin (OPN, Abcam) and tenascin C (TNC, R&D) with primary antibodies all diluted 1:100.

NIH-PA Author Manuscript NIH-PA Author Manuscript NIH-PA Author Manuscript

Human and mouse tissue preparation and immunohistochemistry

5μm mouse sections were stained with Masson's Trichrome using standard protocols. 4μm human and mouse sections were subjected to antigen retrieval: microwaving in EDTA buffer (pH=8.0) for 1 minute for CD36, incubation in Citrate buffer (pH=6.0) at 80°C for 1 hour for CD31 and CD68, or microwaving in citrate buffer (pH=6.0) for 10 minutes for COL1A1 and FN1. Sections were incubated for 1 hour with antibodies to CD36 (Sigma-Aldrich), CD31 (Dako), CD68 (Dako), COL1A1 (Abcam) or FN1 (Epitomics) (diluted 1:100, 1:20, 1:200, 1:500 and 1:250, respectively). Human sections were incubated for 20 minutes with Primary Antibody Enhancer (Thermo Scientific). All sections were incubated for 30 minutes with HRP Polymer (Thermo Scientific), 5 minutes with diaminobenzidine (DAB) and counterstained in Mayer's hematoxylin to visualize nuclei.

Analysis of published microarray data

Microarray datasets GSE6532 and GSE9195 were analyzed using the robust multi-array average method (50). Expression values for each of the five CD36 probe sets were centered by the median then divided by the standard deviation. Linear regression analyses were used to test the associations between the expression of each CD36 probe set and tumor grade, tumor size and age. Data from the probe set that was most strongly associated with tumor grade and tumor size are presented in Supplementary Table S9.

Supplementary Material

Refer to Web version on PubMed Central for supplementary material.

Acknowledgments

We thank members of the Tlsty laboratory, particularly Drs. Colleen Fordyce and Philippe Gascard, for thoughtful discussions, the Nikon Imaging Center (UCSF) for imaging support and Dr. Alfred Au (UCSF), the breast surgeons and Carol Halliday, RN (Aurora Health Care) for providing tissue.

Grant Support

This work was supported by NIH/NCI PO1 CA107584 to T.D.T, K.K., E.Z., and B.P. (under LBNL contract No. DE-AC02-05CH11231), California Breast Cancer Research Program grant 14OB-0165 to T.D.T and NIH/NCI U54 CA143803 to T.D.T. and B.P. (UC Riverside).

References

1. Kalluri R, Zeisberg M. Fibroblasts in cancer. Nat Rev Cancer. 2006; 6:392–401. [PubMed: 16572188]
2. Arendt LM, Rudnick JA, Keller PJ, Kuperwasser C. Stroma in breast development and disease. Semin Cell Dev Biol. 2010; 21:11–18. [PubMed: 19857593]
3. Finak G, Bertos N, Pepin F, Sadekova S, Souleimanova M, Zhao H, et al. Stromal gene expression predicts clinical outcome in breast cancer. Nat Med. 2008; 14:518–527. [PubMed: 18438415]
4. Tlsty TD, Coussens LM. Tumor stroma and regulation of cancer development. Annu Rev Pathol. 2006; 1:119–150. [PubMed: 18039110]
5. Olumi AF, Grossfeld GD, Hayward SW, Carroll PR, Tlsty TD, Cunha GR. Carcinoma-associated fibroblasts direct tumor progression of initiated human prostatic epithelium. Cancer Res. 1999; 59:5002–5011. [PubMed: 10519415]
6. Orimo A, Gupta PB, Sgroi DC, Arenzana-Seisdedos F, Delaunay T, Naeem R, et al. Stromal fibroblasts present in invasive human breast carcinomas promote tumor growth and angiogenesis through elevated SDF-1/CXCL12 secretion. Cell. 2005; 121:335–348. [PubMed: 15882617]
7. Walker RA. The complexities of breast cancer desmoplasia. Breast Cancer Res. 2001; 3:143–145. [PubMed: 11305947]

NIH-PA Author Manuscript

NIH-PA Author Manuscript

NIH-PA Author Manuscript

8. Bing C, Trayhurn P. New insights into adipose tissue atrophy in cancer cachexia. Proc Nutr Soc. 2009; 68:385–392. [PubMed: 19719894]
9. Guo YP, Martin LJ, Hanna W, Banerjee D, Miller N, Fishell E, et al. Growth factors and stromal matrix proteins associated with mammographic densities. Cancer Epidemiol Biomarkers Prev. 2001; 10:243–248. [PubMed: 11303594]
10. Li T, Sun L, Miller N, Nicklee T, Woo J, Hulse-Smith L, et al. The association of measured breast tissue characteristics with mammographic density and other risk factors for breast cancer. Cancer Epidemiol Biomarkers Prev. 2005; 14:343–349. [PubMed: 15734956]
11. Byrne C, Schairer C, Wolfe J, Parekh N, Salane M, Brinton LA, et al. Mammographic features and breast cancer risk: effects with time age, menopause status. J Natl Cancer Inst. 1995; 87:1622–1629. [PubMed: 7563205]
12. Kerlikowske K, Shepherd J, Creasman J, Tice JA, Ziv E, Cummings SR. Are breast density and bone mineral density independent risk factors for breast cancer? J Natl Cancer Inst. 2005; 97:368–374. [PubMed: 15741573]
13. Boyd NF, Byng JW, Jong RA, Fishell EK, Little LE, Miller AB, et al. Quantitative classification of mammographic densities and breast cancer risk: results from the Canadian National Breast Screening Study. J Natl Cancer Inst. 1995; 87:670–675. [PubMed: 7752271]
14. Cummings SR, Tice JA, Bauer S, Browner WS, Cuzick J, Ziv E, et al. Prevention of breast cancer in postmenopausal women: approaches to estimating and reducing risk. J Natl Cancer Inst. 2009; 101:384–398. [PubMed: 19276457]
15. Ziv E, Tice J, Smith-Bindman R, Shepherd J, Cummings S, Kerlikowske K. Mammographic density and estrogen receptor status of breast cancer. Cancer Epidemiol Biomarkers Prev. 2004; 13:2090–2095. [PubMed: 15598766]
16. Boyd NF, Dite GS, Stone J, Gunasekara A, English DR, McCredie MR, et al. Heritability of mammographic density, a risk factor for breast cancer. N Engl J Med. 2002; 347:886–894. [PubMed: 12239257]
17. Ursin G, Lillie EO, Lee E, Cockburn M, Schork NJ, Cozen W, et al. The relative importance of genetics and environment on mammographic density. Cancer Epidemiol Biomarkers Prev. 2009; 18:102–112. [PubMed: 19124487]
18. Chlebowski RT, McTiernan A. Biological significance of interventions that change breast density. J Natl Cancer Inst. 2003; 95:4–5. [PubMed: 12509389]
19. Cuzick J, Warwick J, Pinney E, Duffy SW, Cawthorn S, Howell A, et al. Tamoxifen-induced reduction in mammographic density and breast cancer risk reduction: a nested case-control study. J Natl Cancer Inst. 2011; 103:744–752. [PubMed: 21483019]
20. El-Bastawissi AY, White E, Mandelson MT, Taplin SH. Reproductive and hormonal factors associated with mammographic breast density by age (United States). Cancer Causes Control. 2000; 11:955–963. [PubMed: 11142530]
21. Greendale GA, Reboussin BA, Slone S, Wasilauskas C, Pike MC, Ursin G. Postmenopausal hormone therapy and change in mammographic density. J Natl Cancer Inst. 2003; 95:30–37. [PubMed: 12509398]
22. Haakensen VD, Biong M, Lingjaerde OC, Holmen MM, Frantzen JO, Chen Y, et al. Expression levels of uridine 5' -diphospho-glucuronosyltransferase genes in breast tissue from healthy women are associated with mammographic density. Breast Cancer Res. 2010; 12:R65. [PubMed: 20799965]
23. Yang WT, Lewis MT, Hess K, Wong H, Tsimelzon A, Karadag N, et al. Decreased TGFbeta signaling and increased COX2 expression in high risk women with increased mammographic breast density. Breast Cancer Res Treat. 2010; 119:305–314. [PubMed: 19241157]
24. Vachon CM, Sasano H, Ghosh K, Brandt KR, Watson DA, Reynolds C, et al. Aromatase immunoreactivity is increased in mammographically dense regions of the breast. Breast Cancer Res Treat. 2011; 125:243–252. [PubMed: 20526739]
25. Silverstein RL, Febbraio M. CD36, a scavenger receptor involved in immunity, metabolism, angiogenesis, and behavior. Sci Signal. 2009; 2:re3. [PubMed: 19471024]
26. Chang H, DeFilippis RA, Tlsty TD, Parvin B. Graphical methods for quantifying macromolecules through bright field imaging. Bioinformatics. 2009; 25:1070–1075. [PubMed: 18703588]

NIH-PA Author Manuscript NIH-PA Author Manuscript NIH-PA Author Manuscript

27. Gregoire FM, Smas CM, Sul HS. Understanding adipocyte differentiation. Physiol Rev. 1998; 78:783–809. [PubMed: 9674695]
28. Sfeir Z, Ibrahimi A, Amri E, Grimaldi P, Abumrad N. CD36 antisense expression in 3T3-F442A preadipocytes. Mol Cell Biochem. 1999; 192:3–8. [PubMed: 10331653]
29. Febbraio M, Abumrad NA, Hajjar DP, Sharma K, Cheng W, Pearce SF, et al. A null mutation in murine CD36 reveals an important role in fatty acid and lipoprotein metabolism. J Biol Chem. 1999; 274:19055–19062. [PubMed: 10383407]
30. Yaghjyan L, Colditz GA, Collins LC, Schnitt SJ, Rosner B, Vachon C, et al. Mammographic breast density and subsequent risk of breast cancer in postmenopausal women according to tumor characteristics. J Natl Cancer Inst. 2011; 103:1179–1189. [PubMed: 21795664]
31. Pereira SM, McCormack VA, Hipwell JH, Record C, Wilkinson LS, Moss SM, et al. Localized Fibroglandular Tissue as a Predictor of Future Tumor Location within the Breast. Cancer Epidemiol Biomarkers Prev. 2011; 20:1718–1725. [PubMed: 21693627]
32. Aiello EJ, Buist DS, White E, Porter PL. Association between mammographic breast density and breast cancer tumor characteristics. Cancer Epidemiol Biomarkers Prev. 2005; 14:662–668. [PubMed: 15767347]
33. Kerlikowske K, Cook AJ, Buist DS, Cummings SR, Vachon C, Vacek P, et al. Breast cancer risk by breast density, menopause, and postmenopausal hormone therapy use. J Clin Oncol. 2010; 28:3830–3837. [PubMed: 20644098]
34. Loi S, Haibe-Kains B, Desmedt C, Wirapati P, Lallemand F, Tutt AM, et al. Predicting prognosis using molecular profiling in estrogen receptor-positive breast cancer treated with tamoxifen. BMC Genomics. 2008; 9:239. [PubMed: 18498629]
35. Loi S, Haibe-Kains B, Desmedt C, Lallemand F, Tutt AM, Gillet C, et al. Definition of clinically distinct molecular subtypes in estrogen receptor-positive breast carcinomas through genomic grade. J Clin Oncol. 2007; 25:1239–1246. [PubMed: 17401012]
36. Primo L, Ferrandi C, Roca C, Marchio S, di Blasio L, Alessio M, et al. Identification of CD36 molecular features required for its in vitro angiostatic activity. Faseb J. 2005; 19:1713–1715. [PubMed: 16037098]
37. Jimenez B, Volpert OV, Crawford SE, Febbraio M, Silverstein RL, Bouck N. Signals leading to apoptosis-dependent inhibition of neovascularization by thrombospondin-1. Nat Med. 2000; 6:41–48. [PubMed: 10613822]
38. Kennedy DJ, Kuchibhotla S, Westfall KM, Silverstein RL, Morton RE, Febbraio M. A CD36-dependent pathway enhances macrophage and adipose tissue inflammation and impairs insulin signalling. Cardiovasc Res. 2011; 89:604–613. [PubMed: 21088116]
39. Sica A, Larghi P, Mancino A, Rubino L, Porta C, Totaro MG, et al. Macrophage polarization in tumour progression. Semin Cancer Biol. 2008; 18:349–355. [PubMed: 18467122]
40. McDonnell AM, Robinson BW, Currie AJ. Tumor antigen cross-presentation and the dendritic cell: where it all begins? Clin Dev Immunol. 2010; 2010:539519. [PubMed: 20976125]
41. Landskroner-Eiger S, Qian B, Muise ES, Nawrocki AR, Berger JP, Fine EJ, et al. Proangiogenic contribution of adiponectin toward mammary tumor growth in vivo. Clin Cancer Res. 2009; 15:3265–3276. [PubMed: 19447867]
42. Provenzano PP, Inman DR, Eliceiri KW, Knittel JG, Yan L, Rueden CT, et al. Collagen density promotes mammary tumor initiation and progression. BMC Med. 2008; 6:11. [PubMed: 18442412]
43. Engler AJ, Sen S, Sweeney HL, Discher DE. Matrix elasticity directs stem cell lineage specification. Cell. 2006; 126:677–689. [PubMed: 16923388]
44. Levental KR, Yu H, Kass L, Lakins JN, Egeblad M, Erler JT, et al. Matrix crosslinking forces tumor progression by enhancing integrin signaling. Cell. 2009; 139:891–906. [PubMed: 19931152]
45. Vinals M, Bermudez I, Llaverias G, Alegret M, Sanchez RM, Vazquez-Carrera M, et al. Aspirin increases CD36, SR-BI, and ABCA1 expression in human THP-1 macrophages. Cardiovasc Res. 2005; 66:141–149. [PubMed: 15769457]

NIH-PA Author Manuscript NIH-PA Author Manuscript NIH-PA Author Manuscript

46. Matasic R, Dietz AB, Vuk-Pavlovic S. Dexamethasone inhibits dendritic cell maturation by redirecting differentiation of a subset of cells. J Leukoc Biol. 1999; 66:909–914. [PubMed: 10614771]

47. Ruiz-Velasco N, Dominguez A, Vega MA. Statins upregulate CD36 expression in human monocytes, an effect strengthened when combined with PPAR-gamma ligands Putative contribution of Rho GTPases in statin-induced CD36 expression. Biochem Pharmacol. 2004; 67:303–313. [PubMed: 14698043]

48. Boyer JF, Balard P, Authier H, Faucon B, Bernad J, Mazieres B, et al. Tumor necrosis factor alpha and adalimumab differentially regulate CD36 expression in human monocytes. Arthritis Res Ther. 2007; 9:R22. [PubMed: 17335569]

49. Saibara T, Ogawa Y, Onishi S. Tamoxifen in early breast cancer. Lancet. 1998; 352:404. [PubMed: 9717954]

50. Irizarry RA, Hobbs B, Collin F, Beazer-Barclay YD, Antonellis KJ, Scherf U, et al. Exploration, normalization, and summaries of high density oligonucleotide array probe level data. Biostatistics. 2003; 4:249–264. [PubMed: 12925520]

NIH-PA Author Manuscript
NIH-PA Author Manuscript
NIH-PA Author Manuscript

Significance

CD36 simultaneously controls adipocyte content and matrix accumulation and is coordinately repressed in multiple cell types within tumor and high MD stroma, suggesting that activation of this stromal program is an early event in tumorigenesis. Levels of CD36 and extent of MD are both modifiable factors that provide potential for intervention.

NIH-PA Author Manuscript

NIH-PA Author Manuscript

NIH-PA Author Manuscript

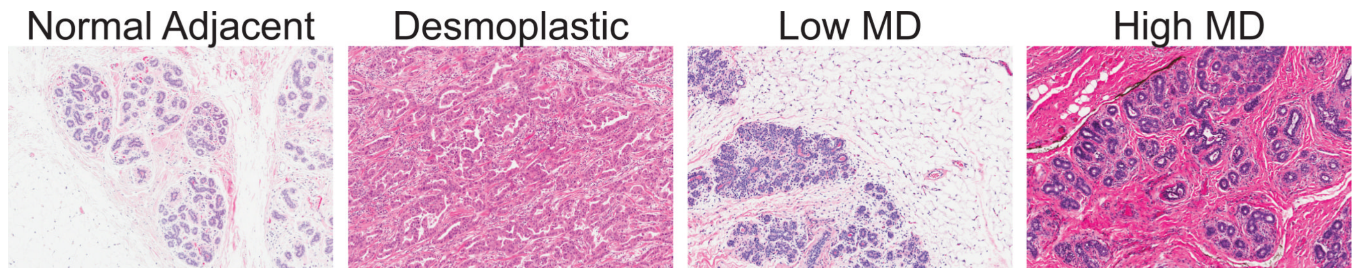

Figure 1. Desmoplasia and tissues with high MD share histologic characteristics
Representative bright field images (×5) of paraffin sections stained with hematoxylin and eosin (Nuclei: blue, ECM: pink, adipocytes: white). Left panels: desmoplastic tissue and histologically normal adjacent tissue from a patient with invasive ductal carcinoma. Right panels: cancer-free tissue from one woman with low MD and one woman with high MD.

NIH-PA Author Manuscript
NIH-PA Author Manuscript
NIH-PA Author Manuscript

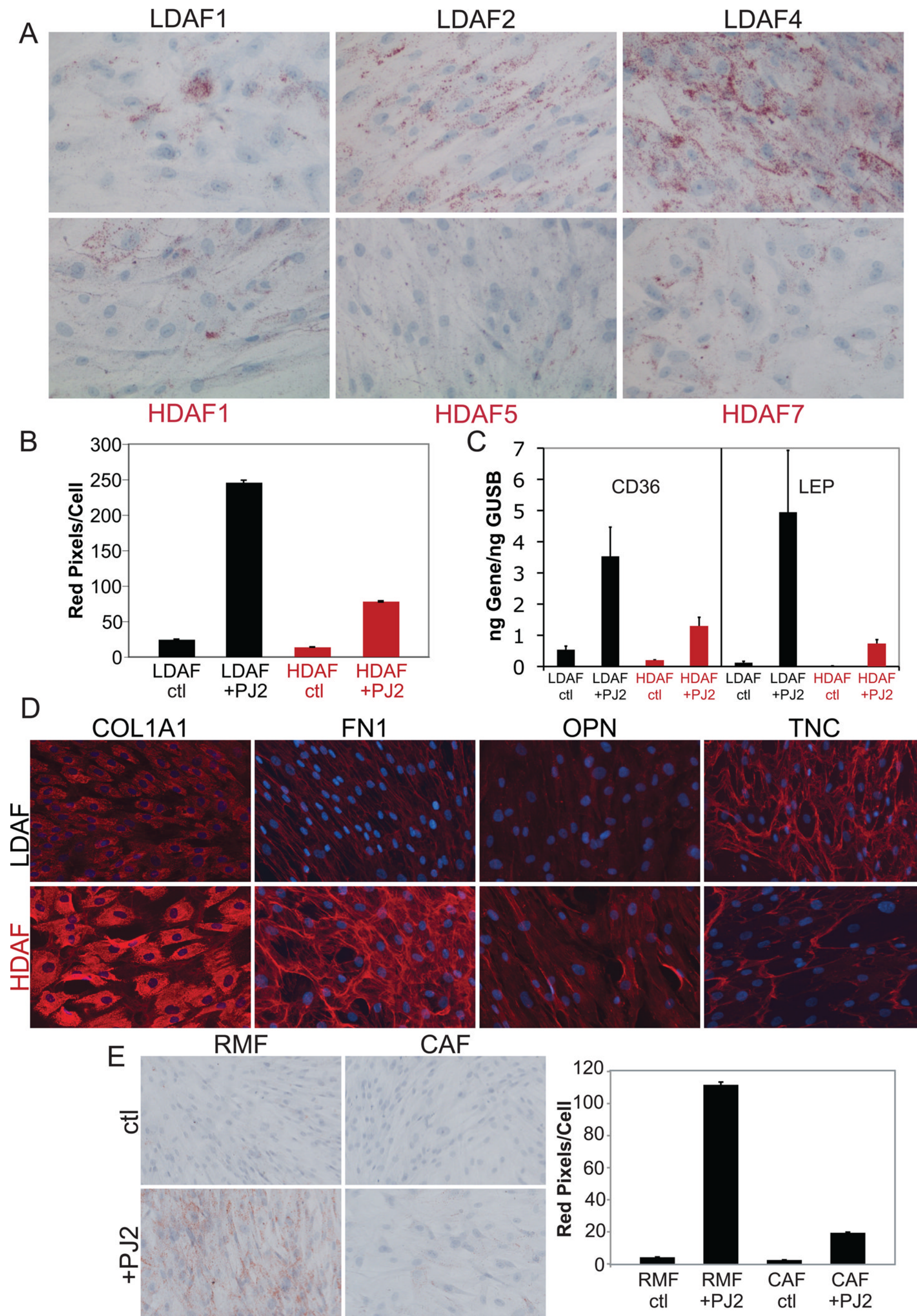

Figure 2. Cultured fibroblasts recapitulate multiple phenotypes associated with their respective tissues of origin

(A) 3 LDAFs and 3 HDAFs were placed under proliferative (ctl) or adipocyte differentiation (+PJ2) conditions for 6 days and assessed for fat accumulation by Oil Red O staining. Representative bright field images (10×) of the fibroblasts under differentiation conditions. **(B)** Average and SEM of Oil Red O staining per cell. **(C)** 4 LDAFs and 4 HDAFs were placed under proliferative (ctl) or adipocyte differentiation conditions (+PJ2) for 2 weeks and assessed for adipocyte differentiation by measuring the expression of genes upregulated in adipogenesis. Average and SEM of CD36 and LEP expression by QPCR (n= 4 for each of 4 LDAFs and 4 HDAFs). **(D)** Representative fluorescent images (10×) highlighting

differential ECM protein deposition in 6 LDAFs and 6 HDAFs grown for 5 days and assessed for accumulation of matrix proteins COL1A1, FN1, OPN and TNC. **(E)** Left panels: representative bright field images (10×) of 1 RMF and 2 CAFs under proliferative (ctl) or adipocyte differentiation (+PJ2) conditions for 7 days and assessed for adipocyte formation by Oil Red O staining. Right panel: average and SEM of Oil Red O staining per cell.

NIH-PA Author Manuscript

NIH-PA Author Manuscript

NIH-PA Author Manuscript

NIH-PA Author Manuscript
NIH-PA Author Manuscript
NIH-PA Author Manuscript

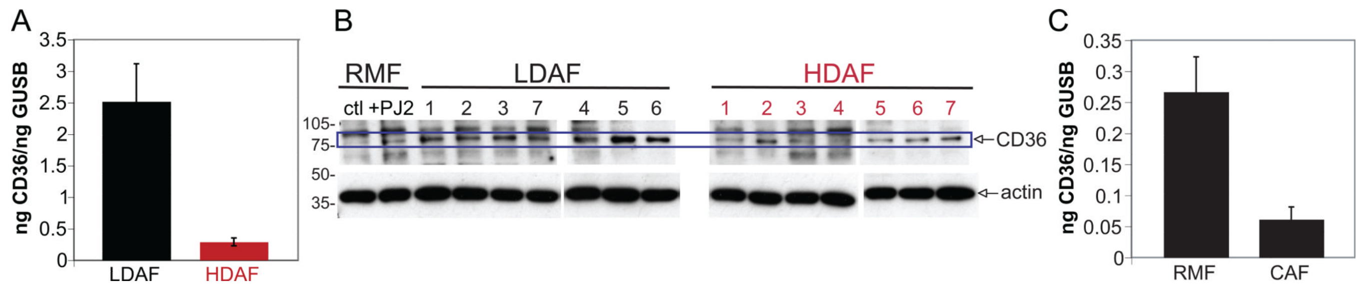

Figure 3. CD36 expression is decreased in HDAFs and CAFs relative to LDAFs and RMFs, respectively

(A) Average and SEM of CD36 expression measured by QPCR (n=3 for each of the 7 LDAFs and 7 HDAFs). **(B)** Western blot analyses for CD36 (top panel), where the arrows indicate CD36 glycosylated state, and actin (lower panel). Positive control for CD36 expression: RMF under proliferative (ctl) or adipocyte differentiation (+PJ2) conditions for 7 days. **(C)** Average and SEM of CD36 expression measured by QPCR (n=3 for each of the 8 RMFs and 8 CAFs).

NIH-PA Author Manuscript
NIH-PA Author Manuscript
NIH-PA Author Manuscript

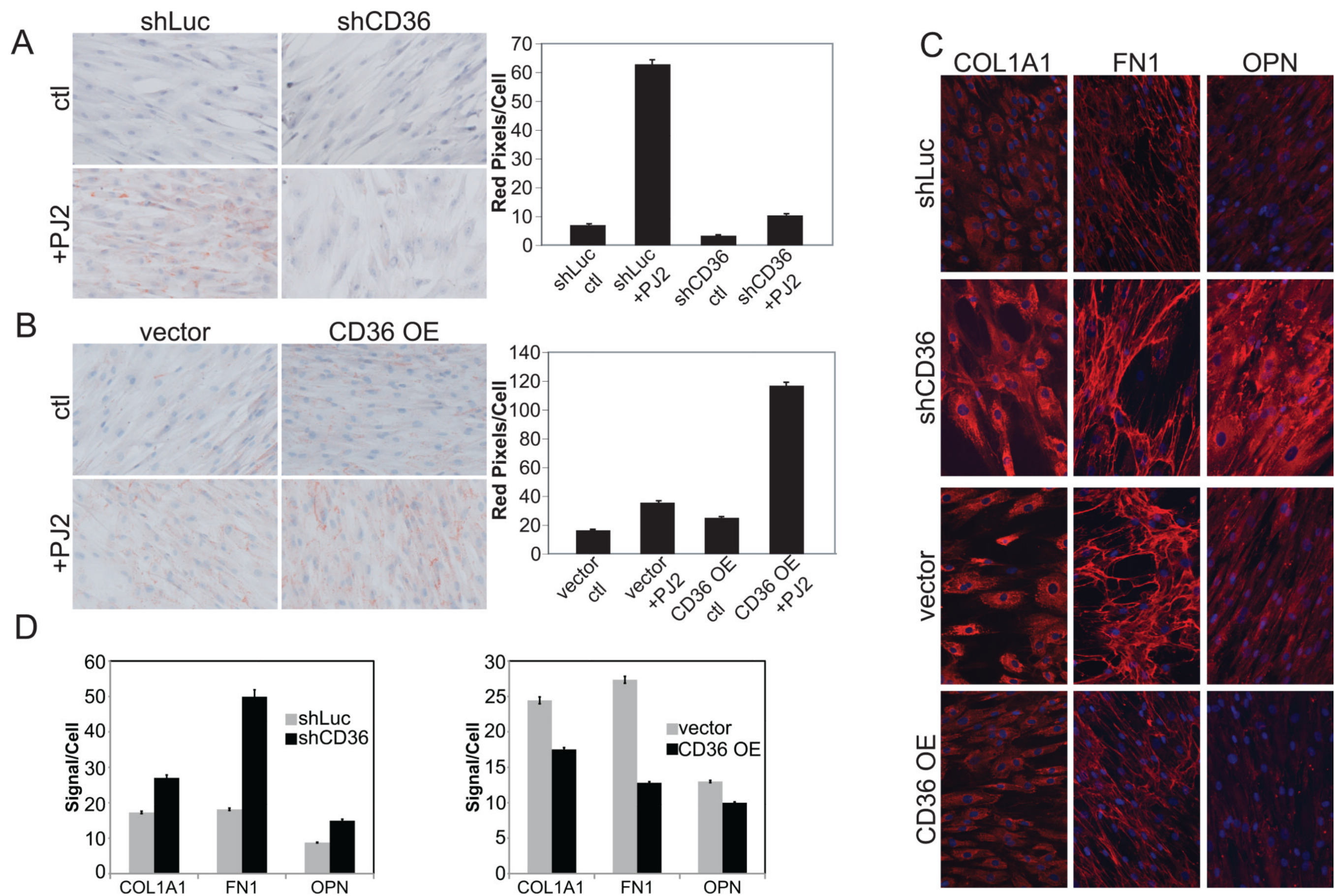

Figure 4. CD36 expression is necessary and sufficient to modulate adipocyte differentiation and matrix accumulation *in vitro*

(A&B: left panels) Representative bright field images (10×) of shLuc, shCD36, vector or CD36 OE cells, under proliferative (ctl) or adipocyte differentiation (+PJ2) conditions for 7 days and assessed for adipocyte formation by Oil Red O staining. **(A&B: right panels)** Average and SEM of Oil Red O staining per cell. **(C)** Representative fluorescent images (10×) of shLuc, shCD36, vector and CD36 OE cells grown for 5 days and assessed for accumulation of matrix proteins COL1A1, FN1 and OPN. **(D)** Average and SEM of staining per cell expressed as signal $\times 10^4$.

NIH-PA Author Manuscript
NIH-PA Author Manuscript
NIH-PA Author Manuscript

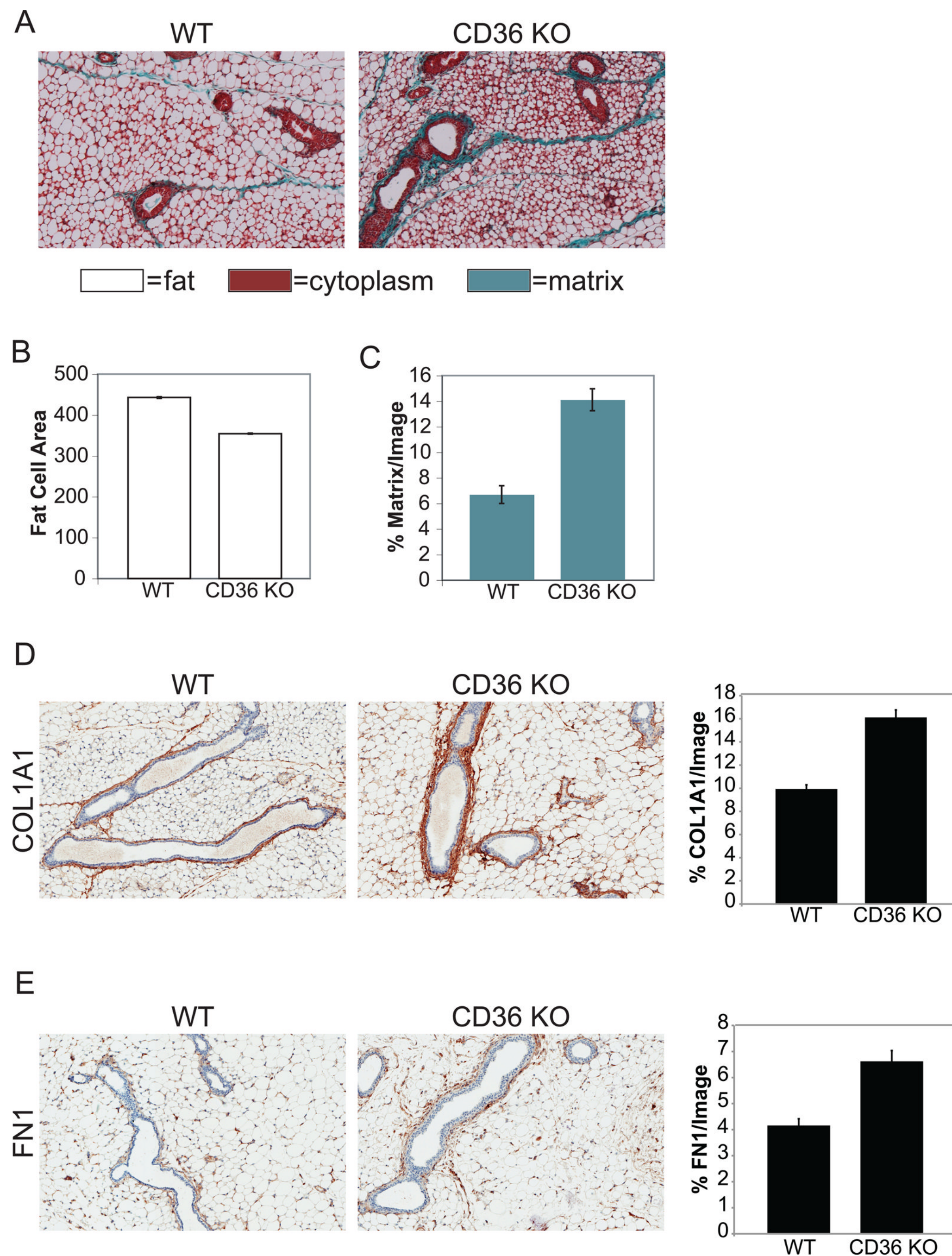

Figure 5. Cd36 knockout mice phenocopy human high MD and desmoplastic tissues
Representative bright field images (10×) of #4 mammary gland paraffin sections from either WT (n=7) or CD36 KO (n=5) mice stained with Masson's Trichrome **(A)**, or for COL1A1 **(D, left panel)** and FN1 **(E, left panel)**. Average and SEM of fat cell area **(B)**, or percent area of either matrix staining **(C)**, COL1A1 staining **(D, right panel)** or FN1 staining **(E, right panel)**.

NIH-PA Author Manuscript

NIH-PA Author Manuscript

NIH-PA Author Manuscript

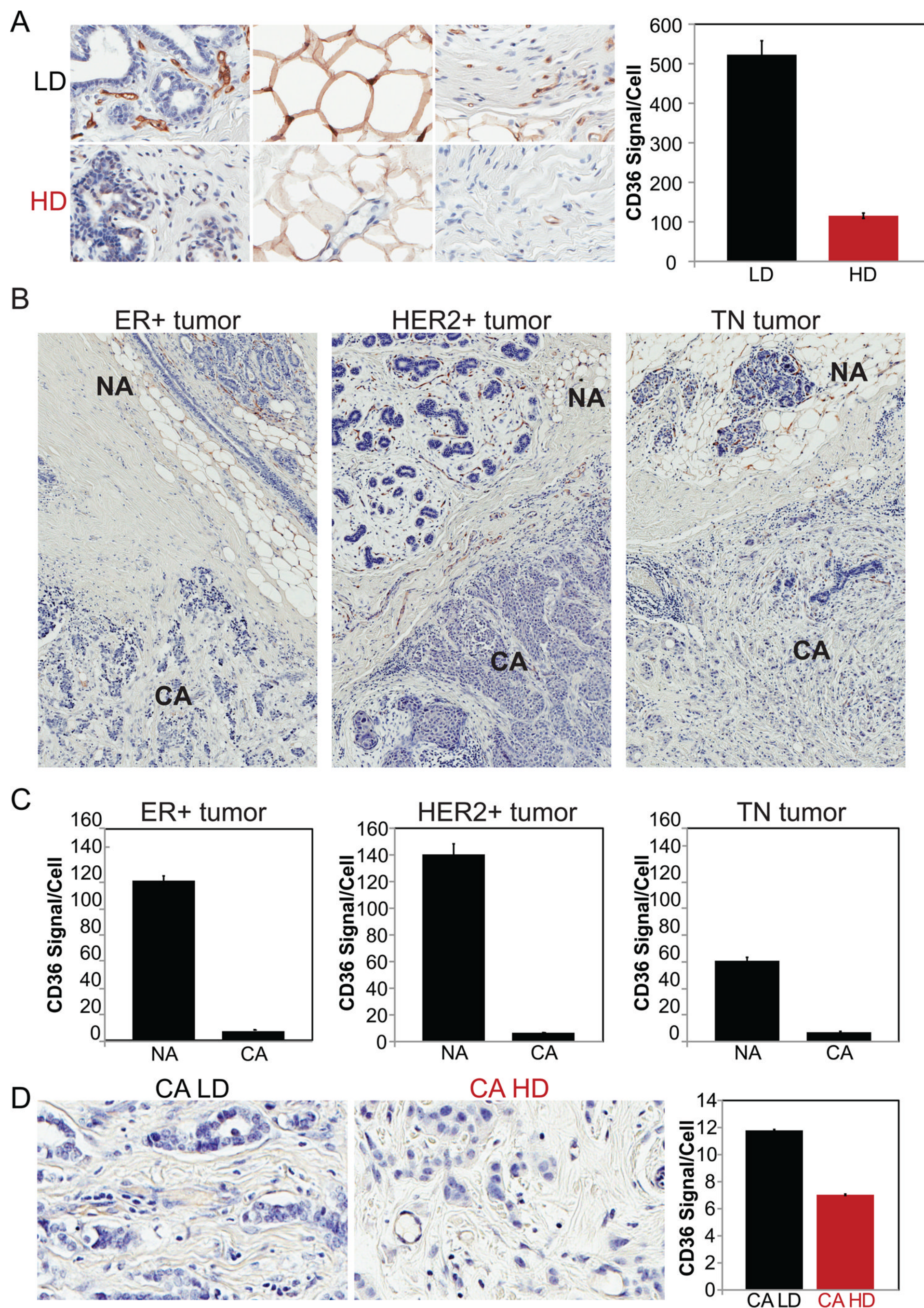

Figure 6. CD36 expression is coordinately regulated in multiple cellular compartments

(A) Left panels: representative bright field images (20×) of paraffin sections from 13 LD and 14 HD tissues stained for CD36. Right panel: average and SEM of CD36 signal per cell. **(B)** Representative bright field images (5×) of paraffin sections with tumor (CA) and normal adjacent (NA) tissue from 8 ER+ tumors, 6 HER2+ tumors and 6 triple negative (TN) tumors stained for CD36. **(C)** Average and SEM of CD36 signal per cell for each tumor subtype. **(D)** Left panels: representative bright field images (20×) of paraffin sections from 21 LD and 14 HD ER+ IDC patients stained for CD36. Right panel: average and SEM of CD36 signal per cell.

NIH-PA Author Manuscript

NIH-PA Author Manuscript

NIH-PA Author Manuscript

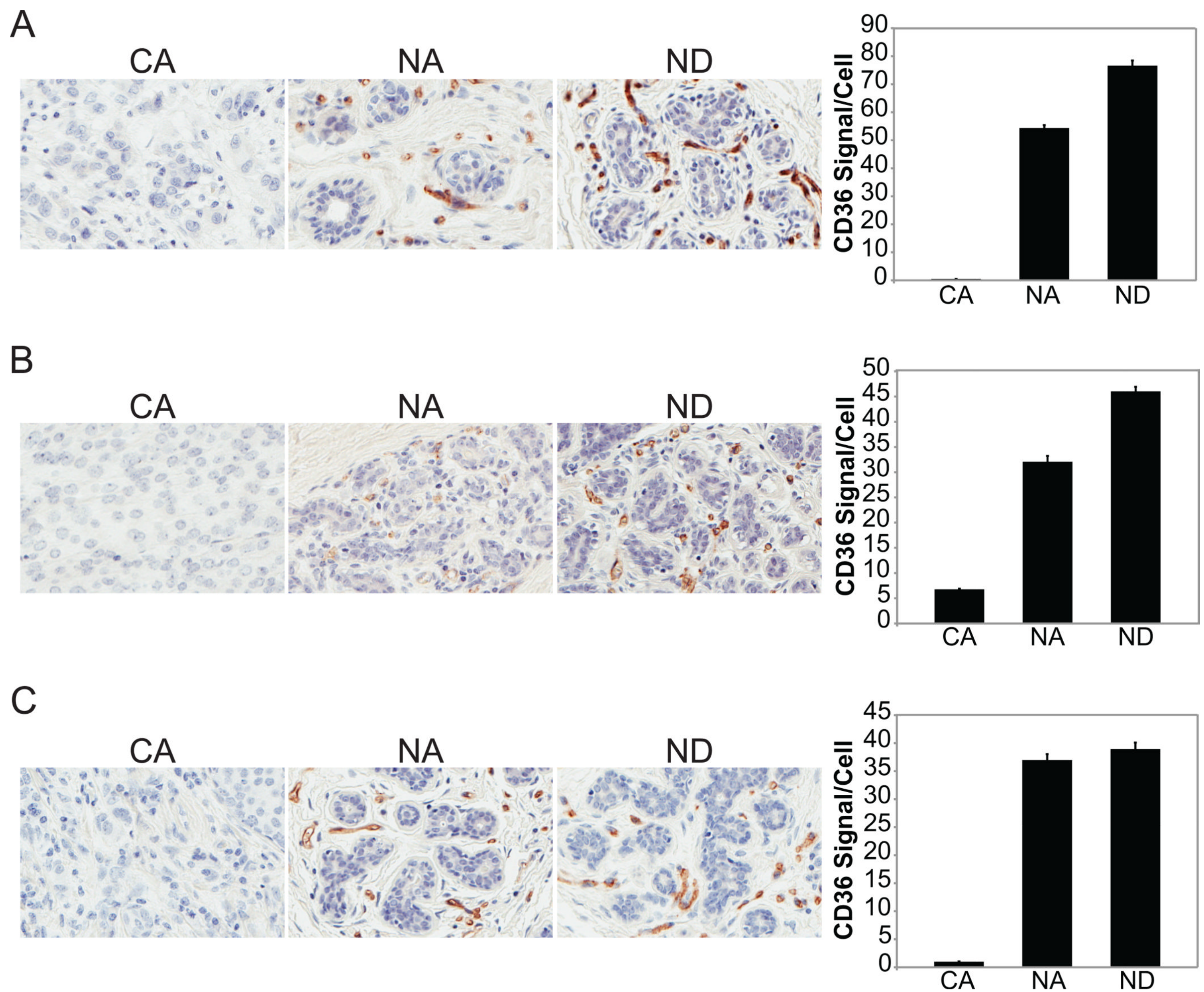

Figure 7. CD36 expression in tissue adjacent and distal to the tumor

(A–C) Left panels: representative bright field images (20×) of paraffin sections with tumor (CA) and normal adjacent (NA) tissue or with normal distal (ND) tissue from 3 mastectomies stained for CD36. Right panels: average and SEM of CD36 signal per cell.